VOL. 13, NO. 7, APRIL 2018 ISSN 1819-6608
ARPN Journal of Engineering and Applied Sciences

www.arpnjournals.com

FORMATION OF A CALCULATION MODEL DETERMINING OPTIMAL RATE OF STOPING FACE MOVEMENT WITH A LARGE DEFORMATION OF A ROCK MASSIF

V. Fomichov, V. Pochepov, V. Sotskov and O. Mamaikin
Department of Underground Mining, National Mining University, Yavornitskogoave, Dnipro, Ukraine
E-Mail: vadymsotskov@gmail.com

ABSTRACT

An effective calculation model of a computational experiment that adequately describes the change in a condition of geotechnical model in time considering the change in geometry of contours of investigated galleries was developed. An analysis of mining-geological and mining-technical conditions of astoping area was carried out. The experience of performing mining and development during a long wall mining method and applied constructive-technological coal extraction schemes, mathematical modeling of geomechanical processes in a geotechnical system was studied. Stress-strain state, manifestations of rock pressure, conditions for maintaining the galleries depending on mining-technical and technological parameters were investigated. Measurements in operating galleries of Dolzhanskaya-Kapitalnaya mine which has similar mining-geological conditions to determine the deformation characteristics of agallerycontour were performed. A calculation model was developed, which was later used to predict a stress-strain state (SSS) of the rock massif in the conditions of Belitskaya mine. The analysis of obtained data allowed determining the values of the optimal rates of stoping face movement, depending on the structure and mechanical characteristics of a coal-bearing rock massif.

Keywords: rockbolt, gallery, rock massif, working face, stope.

INTRODUCTION

Preservation of a stoping gallery in operating condition for the entire period of its use allows reducing production costs, increasing safety and ensuring an increase of intensity of miners' work. At the same time, excessive investments in supporting these galleries lead to an increase in the prime cost of extracted coal. Obtaining optimal technological solutions for galleries drifted in similar mining and geological conditions is facing a number of problems related to both the features of mechanical characteristics of a bearing rock massif and the technologies of installation of tunnel supports available in a particular mine [1].

Currently, there are a large number of methods at a design stage of development that allow determining what type and parameters of the support will be used to support a gallery [2, 3]. A number of such methods operate with formal features and allow obtaining satisfactory design results; others are built on the basis of field observations and interpolate the obtained results onto created objects. However, under conditions when development of the SSS of a geotechnological system occurs under the influence of a number of factors described in a complex manner, such solutions are ineffective. In this case, it is necessary to simulate the gallery condition considering a real combination of various factors affecting its stability. In this case, the model of a computational domain should be optimized considering the results of field observations conducted in similar mining and geological conditions [4].

Problem statement. The purpose of the article is a need to develop a calculation model of a geotechnical system that allows determining geometry changes of amine gallery contour at various rates of a stoping face movement.

During the computational experiment, the following tasks were set: to determine the adequacy of change of the SSS of a support in the simulated computational area for large deformations of the gallery contour; obtain a prediction of condition change of the designed geotechnical system for moving stoping face; to obtain a description of determination of optimal parameters of a rate of movement of a stoping face in examined mining-geological conditions.

The solution of set problems was performed on the basis of a complex approach, including the analysis of mining-geological and mining-technical conditions of stoping site development, generalization of experience in mining and development operations during a long wall mining method and used structural and technological schemes for coal extraction, mathematical modeling of geomechanical processes in a geotechnical system [5].

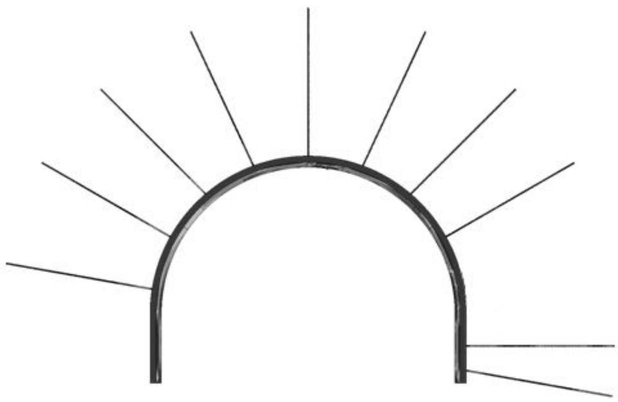

Figure-1. The scheme of installation of rockbolt support selected for calculations.

VOL. 13, NO. 7, APRIL 2018 ISSN 1819-6608
ARPN Journal of Engineering and Applied Sciences

www.arpnjournals.com

Analysis of computational data and field observations. At the first stage of the investigation, in order to determine the optimal scheme for supporting the re-usablegalleries of Belitskayamine the measurements were performed in the galleries of Dolzhanskaya-Kapitalnaya mine that operates in similar mining and geological conditions. The purpose of these measurements was to determine the deformation characteristics of a gallery contour. Then, on the basis of obtained data, a calculation model [6, 7] was calibrated, which was then used to predict the SSS of the bearing rock massif in conditions of Belitskaya mine. To verify and confirm the adequacy of this model, a calculation was performed on the basis of an existing gallery, in which stress sensors were installed on the rockboltsat a distance of 30-50 m from each other. The measurements were performed in real time and were summarized into the graphs shown below. The selected scheme for installing the rockbolting is shown in Figure-1. The graphs in Figures 2-4 were formed according to it.

From the point of view of qualitative changes in the maximum reduced stresses [8], the rockbolts installed in the berm of the drift (Figure-2) pose the greatest interest. When comparing actual and calculated values for the upper rockbolt, it is immediately evident that the second ones qualitatively repeat the first and exceed them by an average of 7-8% of their absolute values. The stress drop in the area of a zero point of the graph is determined by a qualitative change in operating conditions of rockbolts and for upper rockbolts these changes are more distinguished. For lower rockbolts we have a different picture. The calculated stresses are smaller than the results of measurements and in the area of a zero point of passing the stoping face there is a significant divergence of operating modes of rockbolts. However, the magnitude of gradients of these measurements is negligible, and the shift of the inflection point of calculated stresses graph further from a zero point is obviously caused by the absence of stratification modeling of floor rocks at high gradients of their heaving speed.

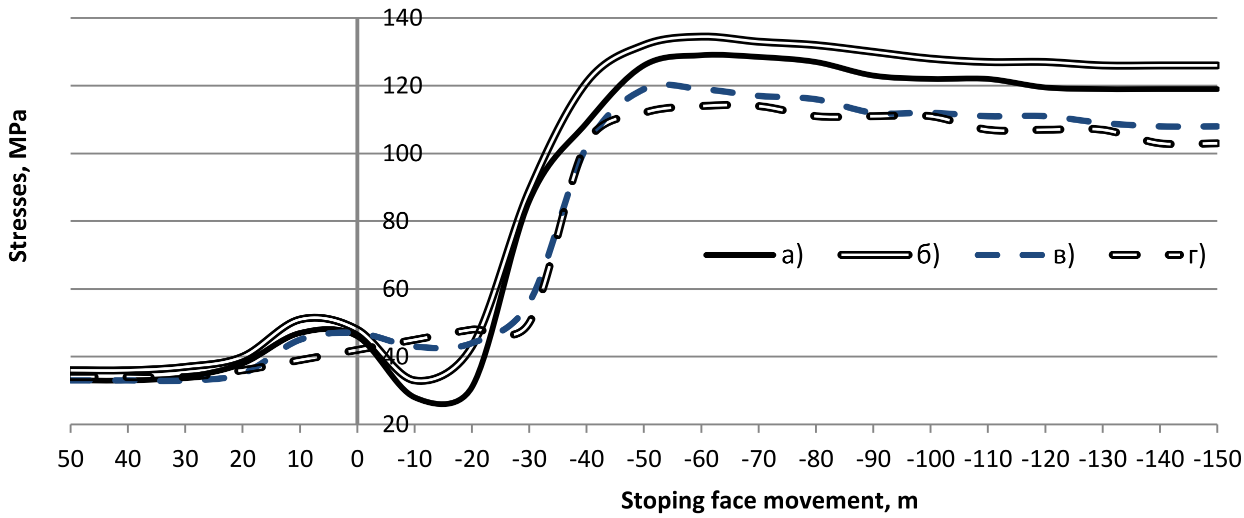

Figure-2. Change of the stressed state of rockbolts installed in a berm of a gallery: (a) actual and (b) calculated values of upper bolts, and (c) actual and d) calculated values of lower bolts.

VOL. 13, NO. 7, APRIL 2018 ISSN 1819-6608
ARPN Journal of Engineering and Applied Sciences

www.arpnjournals.com

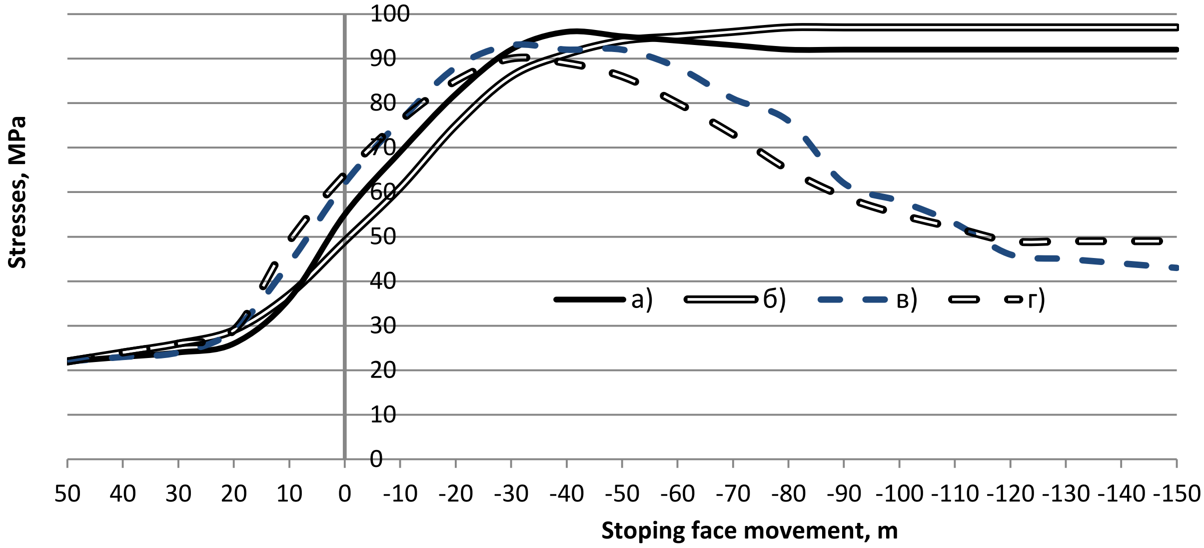

Figure-3. Change of the stress state of rockbolts located below the locks of frame support, a) actual and b) calculated values for the rockbolt from the side of an untouched massif, and c) actual and d) calculated values for the rockbolt on the side of the stoping face.

After passing the stoping face, at a distance of more than 60 m from it, a step-like characteristic of stress drop in rockbolts is observed. This feature can be seen both in natural measurements and in results of calculations. As already indicated, this calculation model was implemented considering the rheology of the rocks, which was necessary for given mining and geological conditions. The observed ledges represent the reaction of rockbolts to the lowering of the main roof caused by the movement of the stoping face.

The proposed calculation model of rockbolt support is designed with a high degree of accuracy, since total deviations of calculated and actual data for both rockbolts are in a range of 2-5%, which is completely within the range of a computational error.

The frame rockbolts located below the locks were combined into the second group of analysis of internal forces. The analysis is based on the stress charts shown in Figure-3.

Prior to stoping face distancing from the calculated point to a distance of more than 50 m, the operation modes of considered rockbolts, both from the untouched massif and from the stoping side, coincide. For a rockbolt installed on the side of the stoping face, the quantitative deviations in calculated and measured data are within 6%. For the opposite rockbolt - deviations reach 16%. After passing this point, the load on the rockbolt from the side of an untouched massif stabilizes.

Simultaneously, the rockbolt installed in the direction of the gallery, perceives less stresses. The patterns of change of stress peaks qualitatively differ in the calculation and measurements of this rockbolt. Absolute deviations of obtained values exceed 19%, which indicates a qualitative description of the condition of rock massif during the computational experiment. In the calculation model, it was not possible to fully describe all the features of development of deformations of the ‘rock massif-support-security structure’ system in time. Discrepancies in values of calculations and measurements appear only in a segment between -50 to -80 m. This indicates the insignificant discrepancies in accepted constraints for a calculation model.

In Figure-4 rockbolt (first), installed from the side of an untouched massif and arockbolt (second), installed towards the gallery, operate in different modes. When the first rockbolt does not yet take the load from the rock massif, the second is in the zone of increased rock pressure before approaching the stoping face. At the same time, its loading and unloading occur spasmodically, but with significantly smaller absolute values than the rockbolt installed in the direction of an untouched rock massif [9].

For the first rockbolt, the calculated and actual stress values coincide qualitatively and quantitatively. The absolute deviation of obtained results is within 11%, but with stoping face distancing from the plane of measuring station the separation occurs for a patternof change in the stress maximum for actual and calculated values. The calculation shows an increase in stresses, and measurements in the mine show insignificant decrease in their maximum in the rockbolt body. This feature is obviously caused by orientation and location of the boundary of limiting condition of rocks of the near-contourrock massif [10]. Obviously, for the computational area, this boundary turned out to be closer to the contour of the re-usable gallery.

ARPN Journal of Engineering and Applied Sciences

www.arpnjournals.com

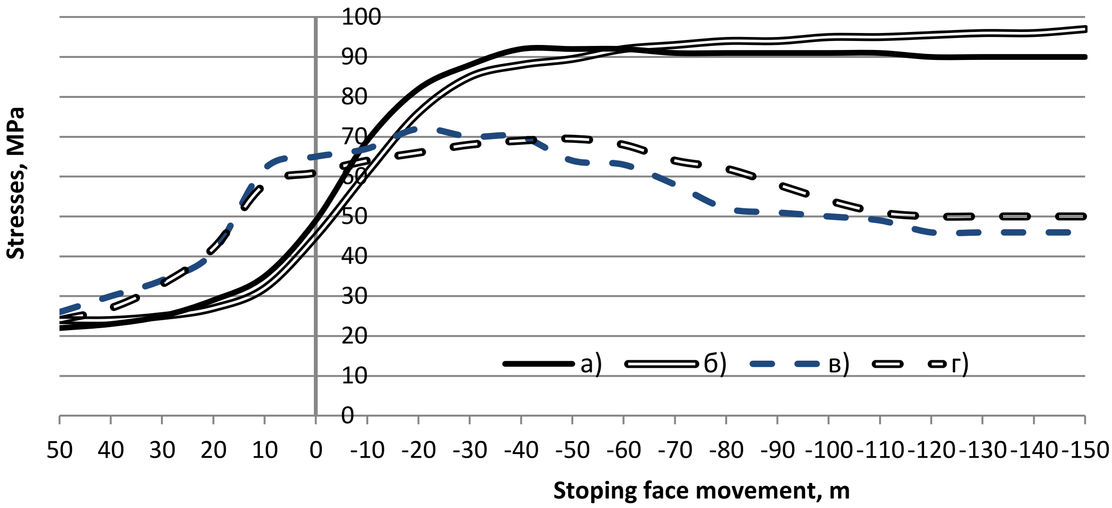

Figure-4. Change in the stress state of rockbolts installed next to the central one, a) actual and b) calculated values for the rockbolt from the side of an untouched massif and c) actual and d) calculated values for the rockbolt from the side of stoping face

Carrying out the computational experiment. Now proceed to the next stage of the study, where we implement the calculation model in predicting the condition change of a junction of stopes during a stoping face movement. Obtained characteristics of a computational area are applicable to the simulation of the SSS of junction of stopes, which arises under the influence of stoping face movement in the conditions of Belitskaya mine [11].

The calculation was performed in two steps. During the first step, the elastoplastic problem was solved, and during the second step, based on the obtained stress-strain state, calculations were made considering the rheological curves obtained experimentally [12]. These data on the structure are matching well with the second model of material flow ability in ANSYS Time Hardening program [9], which is described by the following expression

$$\dot{\varepsilon} = C_1 \cdot \sigma^{C_2} \cdot t^{C_3}, \qquad (1)$$

where $\dot{\varepsilon}$ - equivalent plastic deformations; C_1, C_2, C_3 - experimentally determined coefficients showing the change in the system's SSS depending on material characteristics, the value of equivalent stresses and the current estimated time t .

Analysis of the results. Figure-5 shows the stress intensity distribution σ on the planes of a three-dimensional model corresponding to the plane of a vertical axis of drift symmetry and the plane of the stoping face. Comparison of Figure-5, a and Figure-5, ballows drawing a conclusion about qualitative and quantitative changes in the SSS of a rock massif. In the second case, the stresses are concentrated in the rock layer supporting the main roof of the stoping face and in the side of the gallery; that is, over time the unloading of the near-contour rock massif occurs and at the time presented in Figure-5b, conditions arise for the destruction of the next rock layer in a roof of the stoping face. In this case, the zone of an increased rock pressure in front of the stope completely disappears, and the stresses in the drift behind the stope begin to fall by the value of 8-12 MPa.

ARPN Journal of Engineering and Applied Sciences

www.arpnjournals.com

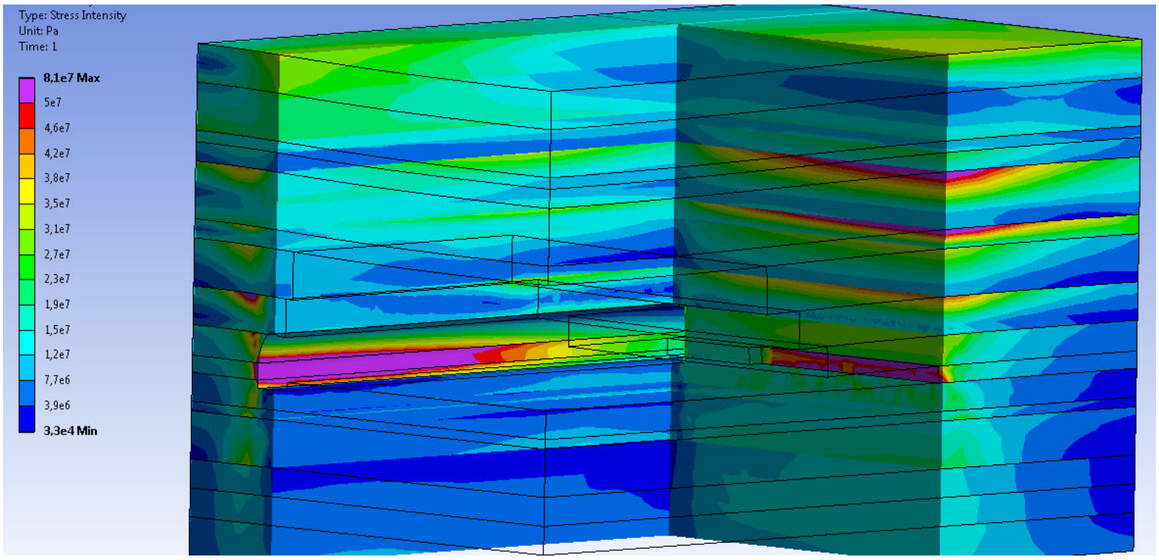

(a)

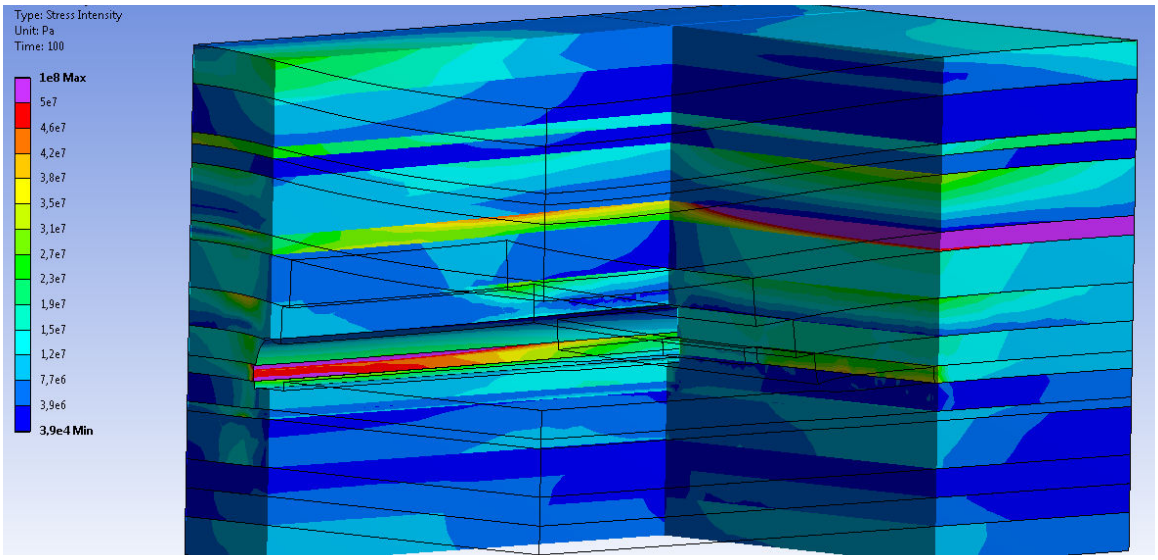

(b)

Figure-5. Stress intensity σ diagrams obtained: (a) at the end of the first step of calculation (elastoplastic setting) and (b) at the time of 100 daysconsidering the rheology of the rocks (the second step)

As a result of performed calculations, the stress intensity distribution σ on the planes of a three-dimensional model corresponding to the plane of a vertical axis of drift symmetry and the plane of the stopingface was shown. Comparison of final results of elastoplastic calculation and calculation considering the time factor immediately allows drawing a conclusion about qualitative and quantitative changes in the stress-strain state of the rock massif. In the second case, the stresses are concentrated in the rock layer supporting the main body of the stopingface and in the side of the gallery, that is, over time the unloading of the rock massif occurs and at the moment of 100 days, conditions arise for the destruction of the next rock layer at the top of the extraction face. In this case, the zone of increased rock pressure in front of the face completely disappears, and the stresses in the drift behind the face begin to fall by an amount of 8-12 MPa.

Thus, consideration of rheology of the rocks during the computational experiment in presented mining and geological conditions allows describing the condition of the geotechnical system when the zone of increased rock pressure changes. This ensures maximum compliance of the computational area with modern concepts of formation and development of zones of rock collapsing near to the face [2, 10].

The most characteristic of obtained results are the diagrams of vertical stress distribution σ_y (Figure-6). First, the dominant stresses of the rock massif in vertical direction are compressive, the gradient of which practically does not depend on stratification of the massif. Secondly, small zones of tensile stresses are formed along the axis of the gallery in the roof and on the floor.

ARPN Journal of Engineering and Applied Sciences

Over time, the pattern of stresses in the mine floor changes insignificantly: absolute values of stresses are less than 3%; the volume of the zone of tensile stresses is within 1-4%. This indicates a slight impact of rheology of the rock massif in the formation of floor heaving in examined mining and geological conditions. On the other hand, as a result of the elastoplastic calculation, a "wave" of tensile stresses was obtained in the roof of the mine, the peak of which falls on the zone of conjugation of the rock layers of the main roof and the last layer of siltstone collapsed behind the stoping face. Considering the rheology, this feature of the rock massif SSS is not observed on the stress plots σ_y. However, this allows drawing a conclusion that this feature can seriously affect the formation of the discharge cavity in the roof of the gallery at a time close to a moment of collapse of the immediate roof of the stoping face.

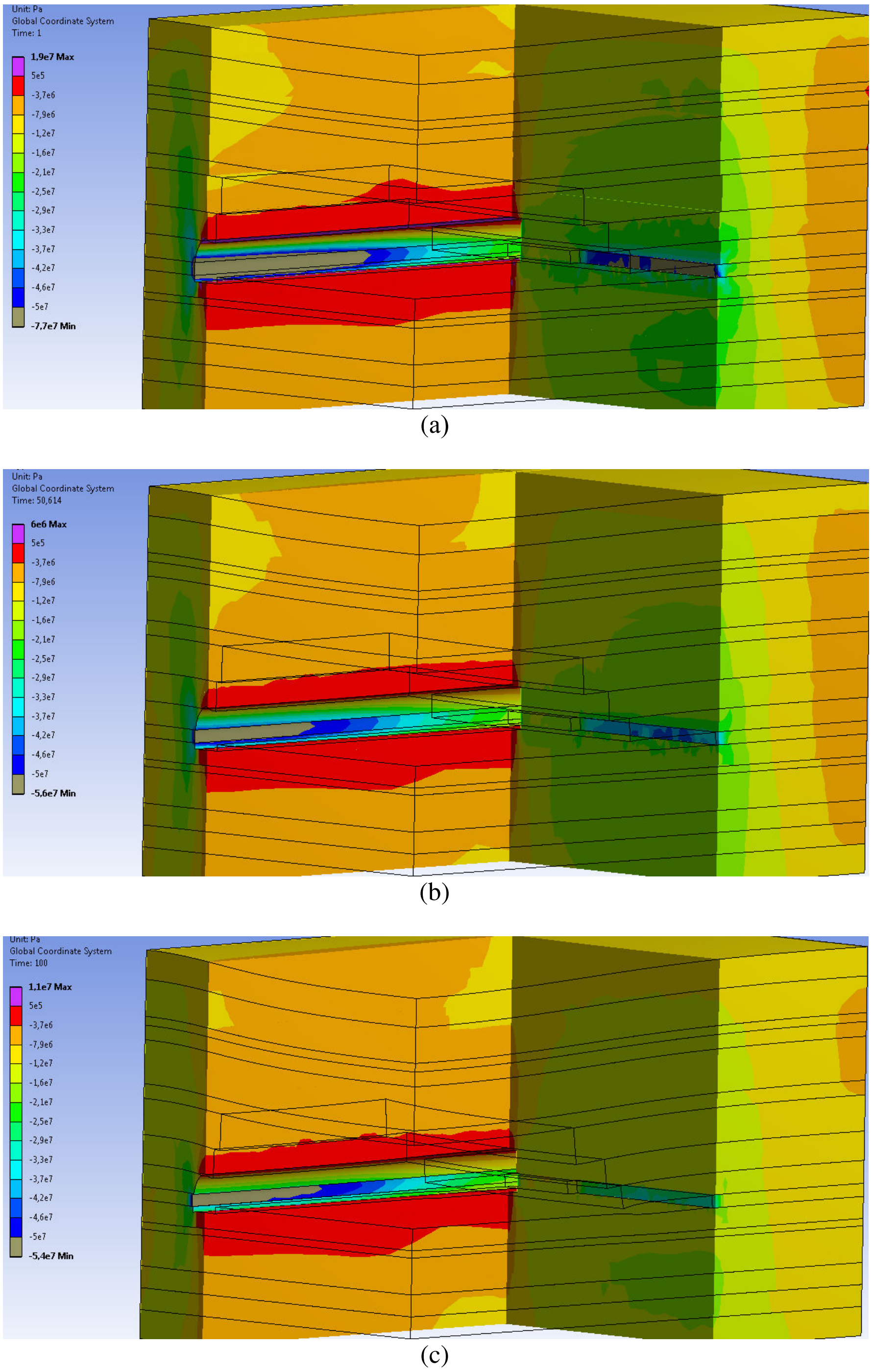

Figure-6. Diagrams of vertical stresses σ_y obtained from the results of calculations: (a) the first step; (b) on the 50^{th} day of the second step; (c) the second step.

ARPN Journal of Engineering and Applied Sciences

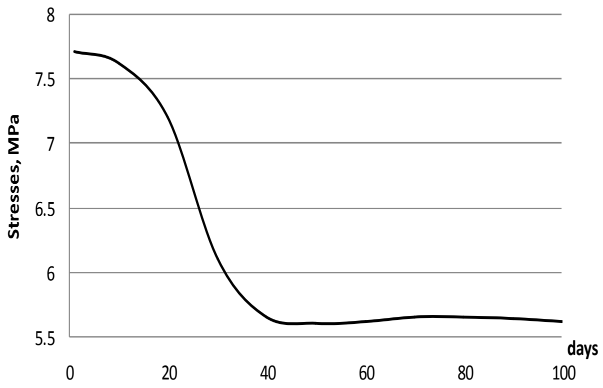

Figure-7. Change in vertical stresses maximum in the model of junction of the stoping gallery and the stoping face with two-step calculations

Now consider the change in vertical stresses maximum σ_y over the entire time interval of the calculation (Figure-7). During the interval of up to 10 days, the maximum stress σ_y remained practically unchanged (within the linear deviation of 1 - 2%), obtained from the calculation of the elastoplastic model. Then a rapid drop of stresses starts and reaches the value of 36%, and starting on the 38th day the stress values stabilize again and do not change significantly until the end of calculation. Therefore, the chosen time interval includes entirely all the main phases of behavior of the rheological medium. This means that the obtained solution is complete in a sense of a physico-mathematical description of the behavior of rocks as a mechanical medium.

Determination of the time point of the limit of effective resistance to vertical deformations in the galleryro of t_0 makes it possible to establish the rate and conditions for installment of support and security systems. The value of this parameter is determined from the following expression.

$$\sigma_y(t_0) = \sigma_y(t_i), \text{if } \frac{\sigma_y(t_{i-1}) - \sigma_y(t_{i+1})}{\sigma_y(t_{max})} < 0.0054 \quad (2)$$

where $\sigma_y(t_{i-1})$, $\sigma_y(t_i)$, $\sigma_y(t_{i+1})$-the values of vertical stresses at the points located sequentially in the graph (see Figure 7) with a fixed increment along the abscissa (days); $\sigma_y(t_{max})$-the maximum value of vertical stresses in the graph shown in Figure-7.

The changes in total displacements obtained at the first and second steps of calculation are of a quantitative nature. At the first step of the calculation, the maximum displacements did not exceed the 0.66 m mark, and then at the end of the second step of calculation they amounted to 2.23 m. At the final phase of rheology calculation, after 70 days, the rate of displacements decreased; the main roof layers collapsed on the rock that fell behind the stopingface. The stress pattern obtained at the end of the calculation indicates that there is no displacement of the coal seam in front of the stopingface. From the side of an untouched massif, the coal seam model demonstrates the tendency to shift into the cavity of the gallery.

Another feature of obtained displacements was qualitative changes in the rocks adjacent to the mechanized support model. First, in the floor rocks, the pillars of the mechanized support are pushed in up to 0.26 m, and secondly, the rock layers hanging over the pillars of the support change their mechanical behavior and begin to deform uncoordinatedly, and this effect is also observed over the stope, although in a much lesser degree. This is due to different values of the coefficient family C_1, C_2, C_3 for a stronger sandstone and a weak siltstone, so that the rheological siltstone curves are more flat with a larger than the sandstone's absolute values in time.

To analyze the emerging feature, the deformation growth graphs shown in Figure-8 were created. It should be noted that, over time, the growth of sandstone deformations are considerably smaller, and changes in the rock layers of siltstone adjacent to it vary considerably. The closer the layer of siltstone is to the rocks of the main roof, the greater the growth of deformations with time is: graph a - maximum 0.25 m; graph b = 0.49. In this case, although the lower layer of siltstone deforms faster its behavior is close to linear and corresponds to the behavior of sandstone, which is understandable, since it is the sandstone that transfers the main load to the model of a given rock layer.

ARPN Journal of Engineering and Applied Sciences

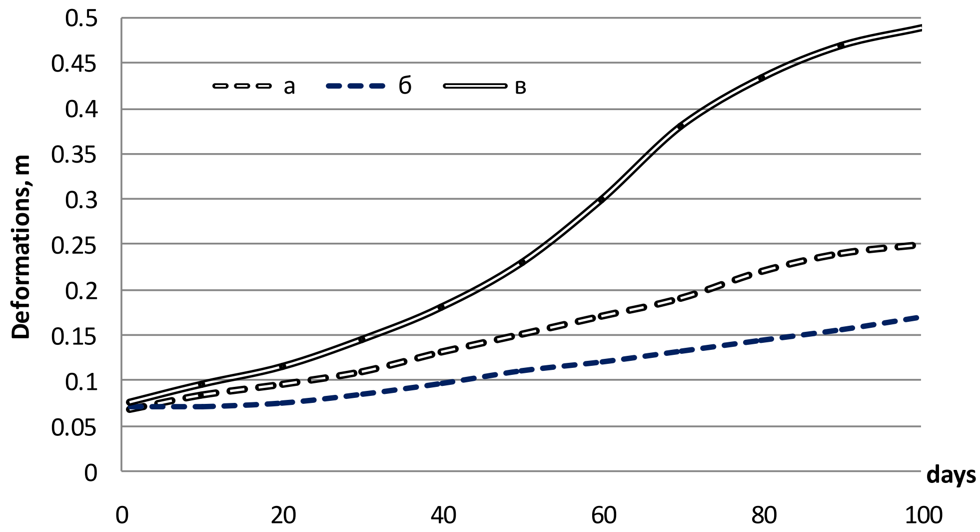

Figure-8. Growth of deformations in the calculation considering rheology in the layers of the main roof of the stope: a) siltstone; b) sandstone; c) top siltstone.

We can distinguish three characteristic zones of the stress-strain state of the rock massif on the graphs presented in Figure-8. The first is characterized by the behavior of the rock massif as a mechanical medium close to the conditions of elastoplastic material. The upper limit of this zone is in arrange of 17-20 days. After that there is a softening of bearing rocks accompanied by an increase in deformations. This process is stopped after day 63-70. Then stabilization occurs, the violation of which can be accompanied by a collapse in a roof of the next rock layer. Predicting the change in behavior of the rock massif allows determining the time point t_{st}, after which intensive softening of the rocks adjacent to the gallery contour stops. The definition of this parameter is based on the following expression

$$\varepsilon(t_{st}) = \varepsilon(t_i), \text{if } \frac{\varepsilon'(t_i)}{\varepsilon'(t_{i+1})} \geq 1.27 \tag{3}$$

where $\varepsilon'(t_i)$, $\varepsilon'(t_{i+1})$-derivatives of the deformation graph at selected points in Figure-8 for a fixed increment along the abscissa axis (days).

The analysis of the above data allows determining the values of optimal rates of movement of astoping face, depending on a structure and mechanical characteristics of a coal-bearing rock massif. In this sense, the condition under which the next rock layer in the immediate top of the face collapses is the presence of a peak of mutual influence of a vertical stress function and a rate of change of these stresses in the current rock layer. This creates a condition for the formation of main cracks that enlarge as a result of stratification of the rock massif along layering planes. As a result, there is a loss of integrity of the rock massif and a formation of a rock block occurs.

The speed of stoping face movement should provide such a technological interval in which the rocks of immediate roof of the stoping face in the area adjacent with the stope remain stable directly behind the stoping face. They are able to carry the load without collapsing on one hand, and are not subjected to increased vertical compressive stresses on the other.

In a course of the studies, the following expression was obtained, which makes it possible to determine an acceptable rate of stoping face movement

$$V = 2{,}17\frac{L_{max}}{T_l} \tag{4}$$

where L_{max}-distance in meters between the stoping face and the maximum of the 'wave' of vertical stresses occurring along the axis of astope (see Figure-6, a); T_l -time interval corresponding to the upper area of stresses in Figure-7.

For the considered solution of the problem of determining the optimal parameters of stability of a junction area of a stopinggallery, the movement rate must be at least 5 m per day.

CONCLUSIONS

When predicting the operational condition of a re-useable stope, the determining factor is the development of deformation of a contour of a rock massif. Consideration of the extreme condition of rock layers makes it possible to obtain a coordinated qualitative (three-phase) and quantitative (averaged deviation is up to 8%) pattern of distribution of internal forces of the geotechnical model. The resulting mathematical expression makes it possible to predict the optimal permissible stoping face movement rate for a selected stope support pattern.

ACKNOWLEDGEMENT

The research is carried out within the framework of scientific topics GP-497 (№0117U006753) "Resource-saving geotechnical and hydrodynamic parametrization of the extraction of low-capacity mineral raw materials in an technogenically loaded environment", financed by the state budget of Ukraine.

REFERENCES

[1] AviDutt. 2011. A new comprehensive method for designing roofrockbolt support system for underground coal mines. Technicaland Geoinformational Systemsin Mining. pp. 317-324.

[2] Fomichov V., Sotskov V. and Malykhin A. 2014. Determination and analysis of the acceptable benchmark changes of the stress strain state of frame and rockbolt fastening elements of dismantling drift when approaching a working face. Naukovyi Visnyk Natsionalnoho Hirnychoho Universytetu. (1): 22-26.

[3] Sotskov V., Demchenko Yu. Salli S. & Dereviahina N. 2017. Optimization of parameters of overworked mining gallery support while carrying out long-wall face workings. Naukovyi Visnyk Natsionalnoho Hirnychoho Universytetu. (6): 34-40.

[4] Salli S., Mamaykin A. & Smolanov S. 2013. Inner potential of technological networks of coal mines. Mining of Mineral Deposits: annual scientific-technical collection. - Netherlands: CRC Press/Balkema. pp. 243-246.

[5] Zienkiewicz O. 2000. The Finite Element Method. R. Taylor. - Vol. 1: The Basic. - Oxford: Butterworth-Heinemann. p. 689.

[6] Rosenblatt J. Bell. S. 1999. Mathematical Analysis for Modeling. Boca Raton: CRC Press LLC. p. 853.

[7] Małkowski P., Niedbalski Z., Majcherczyk T. 2016. Roadway design efficiency indices for hard coal mines. Acta Geodynamicaet Geomaterialia. 13(2): 201-211.

[8] Sidorenko A. and Ivanov V. 2016. Underground mining of multiple seam of coal. ARPN Journal of Engineering and Applied Sciences. 11(7): 4448-4454.

[9] M.Meng Z. Nan, J. Jixiong, Z. Zhicheng. 2017. Numerical Modelling of Mechanical Behavior of Coal Mining Hard Roofs in Different Backfill Ratios: A Case Study. Energies. 10(7): 1-18.

[10] Sotskov V. & Saleev I. 2013. Investigation of the rock massif stress strain state in conditions of the drainage drift overworking. Annual Scientific-Technical Collection - Mining of Mineral Deposits. pp. 197-202.

[11] Saik P.B., Dychkovskyi R.O., Lozynskyi V.G., Malanchuk Z.R. & Malanchuk Ye. Z. 2016. Revisiting the Underground Gasification of Coal Reserves from Contiguous Seams. Naukovyi Visnyk Natsionalnoho Hirnychoho Universytetu. 6, pp. 60-66.

[12] Bondarenko V., Hardygora M., Symanovych H., Sotskov V. & Snihur V. 2016. Numerical methods of geomechanics tasks solution during coal deposits' development. Mining of mineral deposits. 10(3): 1-12.